Intracellular Imaging of HCV RNA and Cellular Lipids by Using Simultaneous Two-Photon Fluorescence and Coherent Anti-Stokes Raman Scattering Microscopies

Xiaolin Nan,[a] Angela M. Tonary,[b] Albert Stolow,[b] X. Sunney Xie,[a] and John Paul Pezacki*[b]

The propagation of HCV requires host–virus interactions that support infection, replication, and viral particle assembly.[1,2] Genotypes 1a and 1b of HCV induce changes in lipid metabolism[3–4] and cause the formation of endoplasmic reticulum (ER)-derived membranous webs on which HCV replicates.[5] HCV also induces the accumulation of lipid droplets (LDs), known as steatosis, on which certain HCV proteins are known to reside.[6–8] Currently, there is no method that permits the observation of spatiotemporal relationships between HCV RNA and alterations in host-cell lipids. Coherent anti-Stokes Raman scattering (CARS) microscopy is a powerful, multiphoton, vibrational imaging modality that is ideal for imaging lipids in live, unstained cells[9,10] and tissues.[11] Selective imaging of lipids is easily achieved by tuning the frequency difference between two pulsed excitation lasers to match the vibrational frequency of the C–H bonds that are abundant in lipids. The use of pulsed, near-IR excitation sources enables the easy combination of CARS with other nonlinear imaging techniques, such as two-photon fluorescence (TPF) microscopy.[12] Herein we establish methods that combine CARS and TPF microscopies to simultaneously examine the subcellular localization of HCV replicon RNA (Figure 1), a noninfectious cell model for HCV replication,[13,14] and changes in lipid phenotype in live Huh-7 hepatoma cells. The approach is also applicable to cell culture models for HCV infection.[15]

First we investigated the localization of LDs in CARS microscopy images of Huh-7 cells that were treated with only the DMRIE-C transfection reagent (mock-transfected). These cells contained LDs that dominated the CH_2 vibrational resonance and corresponded to a size range of 0.3–2 μm (see Figure S1 in the Supporting Information). However, when Huh-7 cells were

[a] X. Nan,+ Prof. X. S. Xie
Department of Chemistry and Chemical Biology, Harvard University
12 Oxford Street, Cambridge, MA 02138 (USA)

[b] Dr. A. M. Tonary,+ Prof. A. Stolow, Prof. J. P. Pezacki
The Steacie Institute for Molecular Sciences
National Research Council of Canada
100 Sussex Drive, Ottawa, K1A 0R6 (Canada)
Fax: (+1)613-952-0068
E-mail: John.Pezacki@nrc-cnrc.gc.ca

[+] These authors contributed equally to this work.

Supporting information for this article is available on the WWW under http://www.chembiochem.org or from the author.

transfected with lipoplexes comprising transfection reagent containing HCV RNA from the pFK-I389luc/NS3-3'/5.1 subgenomic replicon (Figure 1B),[13,14] we observed a trend for increased lipid density in the living cells exposed to HCV RNA as compared to mock-transfected cells (0.35±0.12 vs. 0.25±0.10 a.u., respectively) that was consistent with the initiation of changes in lipid metabolism by the HCV replicon RNA (Figure S1).

To image HCV RNA by TPF, the replicon RNAs were labeled with a two-photon fluorophore (fluorescein) at either the 5′ end of the positive strands, according to Figure 1C, or along the length of the RNA (see the Supporting Information). For simultaneous imaging with combined CARS and TPF microscopies, we used a 711 nm (2 ps) laser beam as both the pump beam for CARS and the excitation beam for TPF. The fluorescein molecules attached to fully labeled and 5′-labeled HCV RNA in lipoplexes were easily probed by TPF, and the fluorescence was stable over a continuous scan of more than five minutes (Figure S2), perhaps due to solid stacking among lipid and RNA molecules in the lipoplexes. We utilized 5′-labeled RNA to study the localization of HCV RNA in Huh-7 cells because activity studies measuring the luciferase genetic reporter demonstrated that 5′-labeled RNA was replication competent (45±17% activity compared to unlabeled RNA), whereas fully labeled RNA was not.

We observed that the HCV RNA–liposome lipoplexes were condensed into tightly packed structures that gave strong TPF signals up to 8 h post-transfection (Figure 2C and D). As previously demonstrated,[3,4] we observed that the HCV RNA localized to the perinuclear region and on or near to LDs/lipoplexes (Figure 2D).

The cells showed a progressive increase in LDs during the first 16 h after transfection, as shown in Figure 2B and D and as quantified in Figure 2E (see the Supporting Information). There was a positive correlation between the density of LDs and the levels of HCV RNA, that is, the cells with the highest density of LDs were also transfected with the highest amount of RNA (Figure 2E). To our knowledge, this is the first detailed, live-cell quantification of total LDs over time in cells expressing HCV RNA and proteins.

At 16 h post-transfection, the fluorescence signals were significantly reduced and more diffuse, and, by 24 h, the 5′-labeled RNA was no longer visible by TPF (Figure 2C). These observations are consistent with the half-life of the labeled RNA. Since replication of the labeled RNA did not involve the incorporation of new fluorophores, our ability to image viral RNA was limited to the lifetime of the fluorescently labeled RNA that was initially delivered to the cells. According to luciferase assays of cellular lysates from Huh-7 cells transfected with unlabeled RNA, the luciferase signal was 100-fold higher in cells transfected with viral RNA than in mock-transfected cells at 2–6 h post-transfection (data not shown). This implies that transfected HCV RNA enters the cells and begins dissociating from liposomes within 2–6 h, followed by translation of encoded viral proteins and replication of the viral RNA. Thus, we believe that the significant increase in LDs observed after 16 h can be attributed directly to the effects of fluorescently labeled RNA
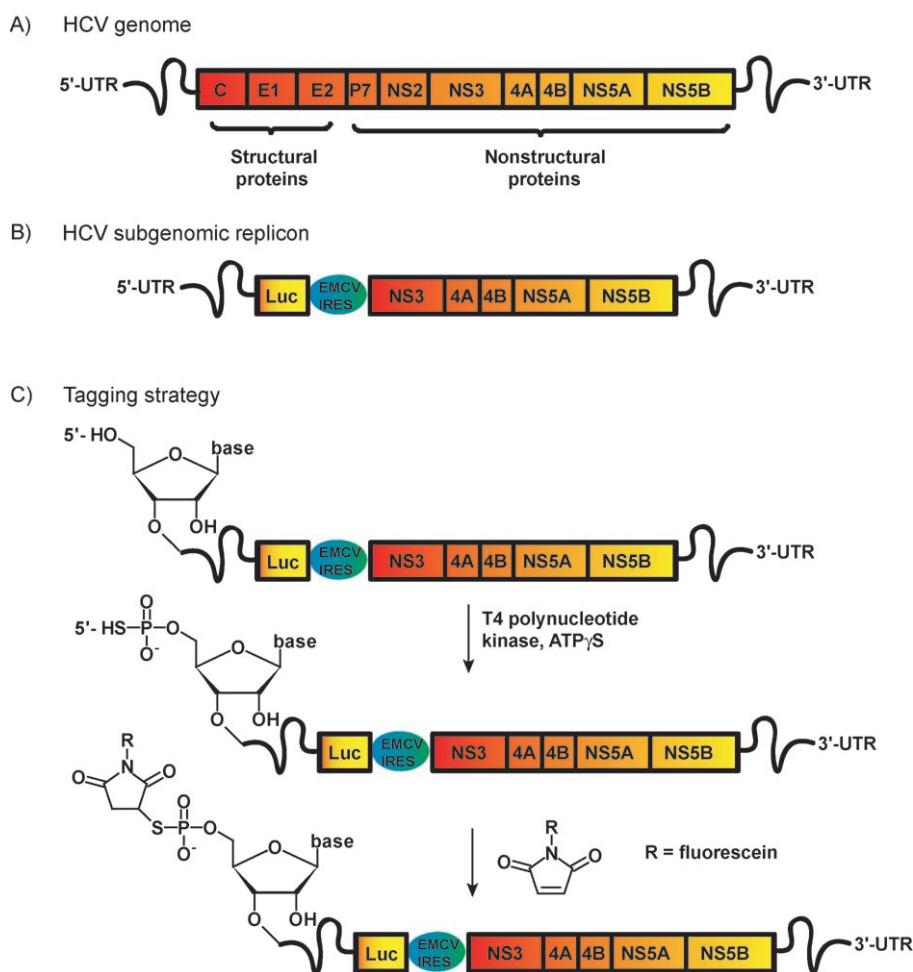
Figure 1. Schematic representations of the HCV RNAs. A) The HCV genome and B) the subgenomic HCV replicon used in this study, and C) the labeling strategy for conjugating a fluorophore to the RNA.

(50 U mL^{-1}), streptomycin (50 µg mL^{-1}, Invitrogen), and 10% with fetal bovine serum (FBS; Cansera, Rexdale, Ontario). The HCV subgenomic replicon plasmid, pFK-I389Luc/NS3–3′/5.1, was kindly provided by Dr. Ralf Bartenschlager (University of Heidelberg, Germany).[16–17] The replicon-containing plasmid consists of a 5′ HCV IRES, the firefly luciferase gene, an EMCV IRES, and the HCV genomic sequences from nonstructural protein-3 (NS3) to the 3′ end of the HCV genome.

Transfection of Huh-7 cells with HCV RNA: Huh-7 cells were seeded in 4.2 cm^2 LabTek chambers (VWR International, Rochester, NY) and were transfected when they reached 70–80% confluency. For transfection, the cells were washed twice with 1X PBS, pH 7.4 (Invitrogen), and once with serum- and antibiotic-free DMEM. The transfection complexes were prepared as follows per chamber: unlabeled or 5′-fluorescein-labeled HCV RNA (1–3 µg) and DMRIE-C reagent (6–18 µL; Invitrogen) were mixed in serum- and antibiotic-free DMEM (500 µL). The lipid–RNA complexes were immediately added to the washed cells and incubated for 2–4 h before either adding DMEM (500 µL supplemented 20% with FBS) to the cells, or removing the media containing complexes and replacing with complete DMEM. Mock-transfected cells were incubated with DMRIE-C in the absence of RNA. Imaging of the transfected cells was carried out 2, 4, 8, 16, and 24 h post-transfection, and the cells were kept on a temperature stage (Harvard Apparatus, Holliston, MA) maintained at 37 °C during imaging.

Simultaneous CARS and TPF microscopies: A laser scanning CARS microscope as previously described[18] was used for simultaneous CARS and TPF imaging. The two excitation sources for CARS, namely the pump and the Stokes beams, were from two synchronized Ti:Sapphire lasers (Tsunami, Spectra Physics, Mountain View, CA) both running at an 80 MHz repetition rate. For imaging lipids by CARS microscopy, the pump and Stokes wavelengths were set at 711 nm and 892 nm, respectively, and the pulse widths were both 2 ps. The two laser beams were collinearly combined and introduced into an Olympus FV300 laser scanning microscope. Depending on the fluorophore of interest, either or both beams could be used for simultaneous TPF imaging.

To achieve better sensitivity of both CARS and TPF, we reduced the repetition rates of both laser beams from 80 MHz to 8 MHz with a pulse picker after the beam combiner. By doing so, we could retain the high peak powers of both beams, which favor nonlinear signal generation, as in CARS and TPF, without increasing the average powers applied to the sample. Typically, for imaging lipids and
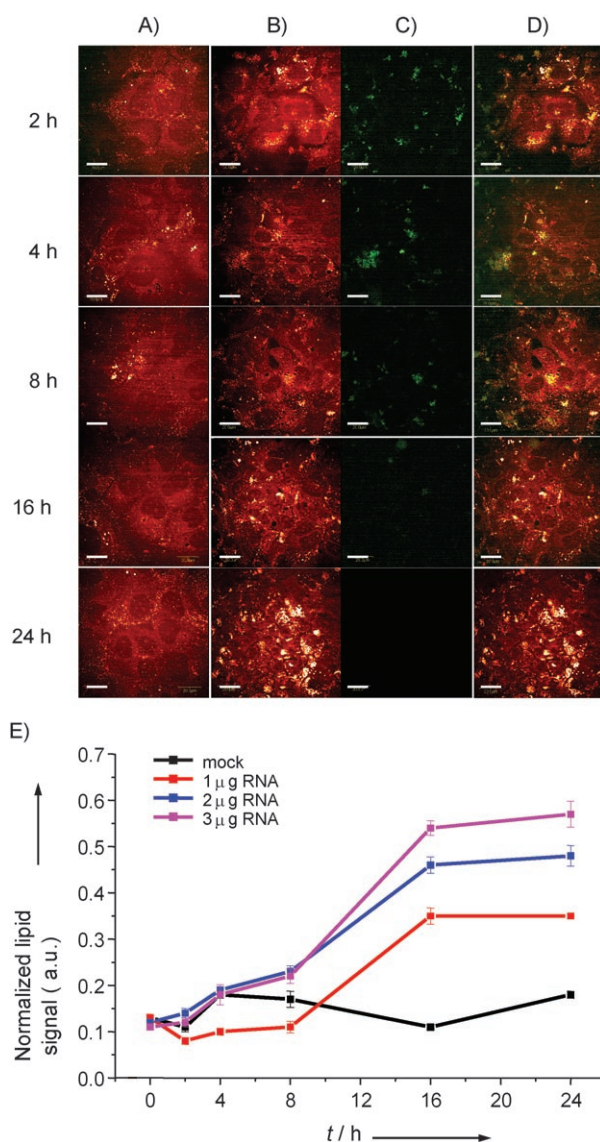
and unlabeled progeny HCV replicon RNA, as well as translated HCV proteins, on host-cell pathways. This conclusion is supported by the fact that mock-transfected cells, which received no viral RNA, showed no accumulation of LDs over the 24 h time period (Figure 2 A and E).

This approach provides a powerful cell-biology tool for: 1) dynamically tracking the subcellular localization of viral RNA under conditions that are not destructive to the cell; and 2) establishing relationships between viral RNA levels and perturbations in host-cell lipid metabolism. Furthermore, we suggest that this approach might be useful for observing viral entry processes and for testing the effects of host and viral genes as well as small-molecule inhibitors on the viral life cycle in real time.

Experimental Section

Cell culture: Huh-7 human hepatoma cells were a kind gift from Dr. Lubica Supekova (The Scripps Research Institute, La Jolla, CA). The cells were cultured in Dulbecco's Modified Eagle Medium (DMEM; Invitrogen, Burlington, Ontario) supplemented with nonessential amino acids (NEAA; 0.1 mM; Invitrogen), penicillin

complete DMEM. Mock-transfected cells were incubated with DMRIE-C in the absence of RNA. Imaging of the transfected cells was carried out 2, 4, 8, 16, and 24 h post-transfection, and the cells were kept on a temperature stage (Harvard Apparatus, Holliston, MA) maintained at 37 °C during imaging.

Figure 2. CARS and TPF imaging of fluorescein-labeled HCV RNA inside cells and quantification of cellular LDs. Huh-7 cells were transfected with 3 µg of 5′-fluorescein-labeled HCV RNA and imaged over 2–24 h. The panels show CARS images of A) mock-transfected cells, and B) CARS, C) TPF, and D) merged images of cells transfected with HCV RNA. Scale bars correspond to 20 µm. E) CARS signals from cellular LDs were quantified from the images of mock-transfected cells and cells transfected with 1–3 µg of 5′-labeled HCV replicon RNA. Each point represents a minimum of 15 random areas and is expressed as the mean ± standard error.

HCV RNA labeled with fluorescein by CARS and TPF, we used 1.5 and 0.5 mW average powers for the pump and Stokes beams, respectively. CARS signals were collected in the forward direction with a 600 ± 20 nm band pass filter stack, and TPF signals were collected in the epi direction with a 500 ± 30 nm filter set.

Estimation of relative lipid content: The CARS signal (I) from cellular lipids was obtained at a Raman shift of 2845 cm^{-1} and contained a resonant signal from lipids (I_R) that interfered with a nonresonant background signal (I_N) and can be written as:

$$I = I_R + I_N + 2\sqrt{I_R I_N} \cos \alpha$$

where α is the phase difference between the resonant and nonresonant signals. Since the largest background signal comes from water, and if we assume that all LDs have similar chemical contents, then the normalized lipid signal is calculated as:

$$\frac{I - I_N}{I_N} = \frac{I_R}{I_N} + 2\sqrt{\frac{I_R}{I_N}} \cos \alpha$$

since it is a monotonic function of I_R/I_N, and I_R/I_N scales up as the lipid content increases. The function I_R/I_N was used rather than I_R in order to reduce the effect from laser power fluctuations. From the images, the overall CARS signal (I) was averaged over random 25×25 µm^2 areas that typically contained one or two cells. The nonresonant CARS signal (I_N) was obtained by averaging the signals in the cell nuclei where there were minimal lipids. Each data point in Figure 2 E represents the mean ± standard error from at least 15 random areas.

Acknowledgements

[1] F. V. Chisari, *Nature* **2005**, *436*, 930 – 932.
[2] K. E. Reed, C. M. Rice, *Curr. Top. Microbiol. Immunol.* **2000**, *242*, 55 – 84.
[3] A. I. Su, J. P. Pezacki, L. Wodicka, A. D. Brideau, L. Supekova, R. Thimme, S. Wieland, J. Bukh, R. H. Purcell, P. G. Schultz, F. V. Chisari, *Proc. Natl. Acad. Sci. USA* **2002**, *99*, 15669 – 15674.
[4] J. Ye, C. Wang R. Sumpter, Jr., M. S. Brown, J. L. Goldstein, M. Gale, Jr., *Proc. Natl. Acad. Sci. USA* **2003**, *100*, 15865 – 15870.
[5] R. Gosert, D. Egger, V. Lohmann, R. Bartenschlager, H. E. Blum, K. Bienz, D. Moradpour, *J. Virol.* **2003**, *77*, 5487 – 5492.
[6] K. Moriya, H. Yotsuyanagi, Y. Shintani, H. Fujie, K. Ishibashi, Y. Matsuura, T. Miyamura, K. Koike, *J. Gen. Virol.* **1997**, *78*, 1527 – 1531.
[7] R. G. Hope, J. McLauchlan, *J. Gen. Virol.* **2000**, *81*, 1913 – 1925.
[8] S. T. Shi, S. J. Polyak, H. Tu, D. R. Taylor, D. R. Gretch, M. M. Lai, *Virology* **2002**, *292*, 198 – 210.
[9] J. X. Cheng, X. S. Xie, *J. Phys. Chem. B* **2004**, *108*, 827 – 840.
[10] X. L. Nan, J. X. Cheng, X. S. Xie, *J. Lipid Res.* **2003**, *44*, 2202 – 2208.
[11] C. L. Evans, E. O. Potma, M. Puoris'haag, D. Côté, C. P. Lin, X. S. Xie, *Proc. Natl. Acad. Sci. USA* **2005**, *102*, 16807 – 16812.
[12] E. O. Potma, X. S. Xie, *ChemPhysChem* **2005**, *6*, 77 – 79.
[13] R. Bartenschlager, V. Lohmann, *Antiviral Res.* **2001**, *52*, 1 – 17.
[14] S. M. Sagan, Y. Rouleau, C. Leggiadro, L. Supekova, P. G. Schultz, A. I. Su, J. P. Pezacki, *Biochem. Cell Biol.* **2006**, *84*, 67 – 79.
[15] J. Zhong, P. Gastaminza, G. Cheng, S. Kapadia, T. Kato, D. R. Burton, S. F. Wieland, S. L. Uprichard, T. Wakita, F. V. Chisari, *Proc. Natl. Acad. Sci. USA* **2005**, *102*, 9294 – 9299.
[16] V. Lohmann, F. Korner, J. O. Koch, U. Herian, L. Theilmann, R. Bartenschlager, *Science* **1999**, *285*, 110 – 113.
[17] B. Rakic, S. M. Sagan, M. Noestheden, S. Bélanger, X. L. Nan, C. L. Evans, X. S. Xie, J. P. Pezacki, *Chem. Biol.* **2006**, *13*, 23 – 30.
[18] X. L. Nan, E. O. Potma, X. S. Xie, *Biophys. J.* **2006**, *91*, 728 – 735.